[redacted]

Copy
RM L54K16

RESEARCH MEMORANDUM

CLASSIFICATION CHANGED TO Unclassified
BY AUTHORITY OF NASA RA# 12
ON 3/16/67 OF JEC

EXPERIMENTAL INVESTIGATION OF AN AXIAL-FLOW SUPERSONIC COMPRESSOR HAVING SHARP LEADING-EDGE BLADES WITH AN 8-PERCENT MEAN THICKNESS-CHORD RATIO

By Theodore J. Goldberg

Langley Aeronautical Laboratory
Langley Field, Va.

[redacted]

NATIONAL ADVISORY COMMITTEE FOR AERONAUTICS

WASHINGTON

February 4, 1955

[redacted]

NATIONAL ADVISORY COMMITTEE FOR AERONAUTICS

RESEARCH MEMORANDUM

EXPERIMENTAL INVESTIGATION OF AN AXIAL-FLOW SUPERSONIC COMPRESSOR HAVING SHARP LEADING-EDGE BLADES WITH AN 8-PERCENT MEAN THICKNESS-CHORD RATIO

By Theodore J. Goldberg

SUMMARY

A 16-inch-diameter rotor with shock-in-rotor-type supersonic-compressor blade sections having sharp leading edges and an 8-percent mean thickness-chord ratio was tested with and without guide vanes.

Although the rotor was designed to operate in air, all tests were made in Freon-12. The compressor was designed for a pressure ratio of 2.6 at a tip speed of 1,600 fps in air (730 fps in Freon-12) with a weight flow of 29 lb/sec of air (54.5 lb/sec of Freon-12). The tests covered a range of tip speed from 485 to 815 fps (65 percent to 110 percent of design speed) which corresponds to a range of 1,050 to 1,760 fps in air.

The rotor with guide vanes produced a total-pressure ratio of 2.06 and an efficiency of 78.6 percent with a weight flow of 51.2 lb/sec of Freon-12 at the design speed of 730 fps. The rotor, operating without guide vanes, produced a pressure ratio of 1.96 and an efficiency of 74.5 percent with a weight flow of 52 lb/sec of Freon-12 at design speed but reached a peak pressure ratio of 2.0 and an efficiency of 81 percent with a weight flow of 51.2 lb/sec of Freon-12 at 95 percent of design speed.

Rounding the leading edges to a 0.010-inch radius decreased the total-pressure ratio, efficiency, and weight flow at all speeds tested except at design speed without guide vanes at which point a higher total-pressure ratio was reached.

Rounding the leading edges decreased the relative total-pressure recovery as a result of changing the shock boundary-layer interaction caused by a changing wave pattern within the blade passage.

INTRODUCTION

In continuing the investigation to develop axial-flow shock-in-rotor-type supersonic compressors having high thickness-chord ratios, a rotor identical in design to that of reference 1 but having sharp leading edges was constructed and tested to substantiate the design technique and to evaluate the effects of a 0.010-inch leading-edge radius on a compressor of this type.

The rotor was designed aerodynamically and structurally to operate in air but all tests were made in Freon-12 because of bearing difficulties. The rotor was designed to produce a pressure ratio of 2.6 at a tip speed of 1,600 fps in air (730 fps in Freon-12) with a weight flow of 29 lb/sec of air (54.5 lb/sec of Freon-12).

This investigation was conducted by the Supersonic Compressor Section of the Langley Compressibility Research Division.

SYMBOLS

a	velocity of sound, fps
M	Mach number, ratio of flow velocity to velocity of sound, V/a
P	total or stagnation pressure, lb/sq ft
p	static pressure, lb/sq ft
T	total or stagnation temperature, $^{\circ}R$
t	static temperature, $^{\circ}R$
ΔT	measured stagnation-temperature rise, $^{\circ}R$
$\Delta T'$	isentropic stagnation-temperature rise, $^{\circ}R$
U	rotational velocity of blade element at any radius, fps
V	velocity of fluid, fps
W	weight flow, lb/sec
W_{open}	weight flow at open throttle, lb/sec
W_{closed}	weight flow at closed throttle, lb/sec

β	angle between axial direction and flow direction, deg (fig. 1)
δ	ratio of actual inlet total pressure to standard sea-level pressure, $P_o/2116$
γ	ratio of specific heats
η	adiabatic efficiency, $\Delta T'/\Delta T$
θ	ratio of actual inlet stagnation temperature to standard sea-level temperature, $T_o/518.4$
ϕ	turning angle, rotor coordinates, deg
ρ	density, slugs/cu ft
P_4/P_2	relative total-pressure recovery
$W\frac{\sqrt{\theta}}{\delta}$	equivalent weight flow, lb/sec
$U_t/\sqrt{\theta}$	equivalent tip speed, fps

Subscripts:

a	axial
t	tip
o	settling chamber
1	rotor entrance, stationary coordinates
2	rotor entrance, rotor coordinates
4	rotor exit, rotor coordinates
5	rotor exit, stationary coordinates

GENERAL AERODYNAMIC DESIGN

The general design specifications for the compressor were identical to those reported in reference 1, but, for the sake of continuity of the present paper, they are outlined as follows:

Rotor Design

Tip diameter, in.	16
Hub-tip diameter ratio	0.75
Axial inlet Mach number at the pitch	0.80
Guide-vane turning	For constant radial M_2 and P_2
Tip speed in air, fps	1,600
Relative exit Mach number at pitch section	0.75
Relative total-pressure loss	Normal shock loss for M_2
Rotor turning at pitch, deg	16
Absolute exit Mach numbers	Subsonic
Tip and root ϕ and M_5	To satisfy radial equilibrium

The velocity diagrams for this design are presented in figure 1.

Blade-Section Design

The supersonic portion of the blade sections was designed by the two-dimensional characteristic method as described in references 1 and 2 and is shown in figure 2. In order to obtain a high thickness-chord ratio, the blades were designed with a maximum of supersonic turning for the chosen wedge angle, contraction ratio, and family of expansion waves cancelled on the opposite surface. (See fig. 2.) In the rearward portion of the blade, a large rate of area growth (equivalent to a 7° conical expansion angle) was provided for subsonic diffusion. The solidity was held to about 2.5.

APPARATUS AND METHODS

The apparatus and methods were similar to those used and discussed in reference 1 and are outlined as follows:

The compressor test rig (shown schematically in fig. 3) was designed in accordance with NACA standards (ref. 3). The rotor was driven through a 2:1 gear-ratio speed increaser by a 3,000-horsepower induction motor which was driven by a variable-frequency power supply.

The rotor was designed for 46 blades which were machined from 75S-T aluminum alloy and wire-locked in a $2\frac{1}{32}$-inch-wide rotor hub which was machined from 14S-T aluminum alloy. A photograph of the test rotor appears in figure 4.

Twenty cast tin-bismuth guide vanes having a solidity of 1.5 were used upstream of the rotor where the annulus area was $14\frac{1}{4}$ percent greater than that immediately ahead of the rotor in order to reduce the possibility of choking the flow at the vanes.

The same pitot-static-yaw survey probe and shielded total-pressure and total-temperature rakes were located in the identical positions as for tests with the rounded leading-edge rotor in order to attribute any differences in the results between the two rotors to effects generated by the differences in the leading edge.

Tests were made in Freon-12 over a range of tip speed from about 30 percent below design to about 10 percent above design. The settling-chamber pressures varied from about 0.4 atmosphere for high-speed tests to about 0.8 atmosphere for low-speed tests with a corresponding variation of test gas purity from about 93 to 97 percent by volume of Freon-12. The values of the gas properties corresponding to the purity measured for each test were used in the performance calculations.

The rotor characteristics were determined from an arithmetical average of temperature and pressure measurements obtained from fixed rakes; whereas for radial survey tests, results of measurements by temperature rakes and the pitot-static-yaw survey probe were mass weighted to yield average values. All values of weight flow presented are those measured by a calibrated Venturi tube. All values of efficiency presented are those based upon temperature-rise measurements rather than upon momentum-change measurements across the rotor. The latter efficiency was consistently higher by about 4 percent.

RESULTS AND DISCUSSION

Rotor With Guide Vanes

<u>Overall performance</u>.- The overall performance of the rotor operating with guide vanes over a range of equivalent tip speed from 30 percent below design to 10 percent above design is presented in figure 5 in terms of adiabatic efficiency and equivalent weight flow as functions of total-pressure ratio at constant speeds. At the design tip speed of 730 fps, a total-pressure ratio of 2.06 at an efficiency of 78.6 percent and a weight flow of 51.2 lb/sec of Freon-12 were measured.

At design speed the weight flow was affected by back pressure (fig. 5(b)) decreasing at a pressure ratio of about 1.72 and then increasing with a further increase of back pressure until the same weight flow as the open throttle condition was reached. Normally, a decrease in weight flow with throttle for a supersonic compressor indicates an unstarted condition. However, the fact that the weight flow again increased with further back pressure and reached the value for open throttle indicates that a started condition did exist. There was a drop and then an increase in efficiency (fig. 5(a)) at the same total-pressure ratio corresponding to this change in weight flow. The same results were obtained from many tests during which there was no noise to indicate a partial stall or other peculiarity. This effect also occurred at a speed of 5 percent above design but here the weight flow did not again reach as high a value as for the open-throttle condition. However, at a speed of 10 percent above design, once the weight flow decreased with back pressure it continued to fall until the rotor stalled. At speeds above design both the pressure ratio and efficiency fell off very sharply. These peculiarities in the characteristic curves at and above design speed are not understood but may be connected in some way with shock boundary-layer interaction within the blade passages which in turn could affect the entering flow.

Rotor-blade-element performance.- Variations of several rotor parameters at design speed and maximum efficiency as functions of radial position are presented in figure 6. The estimated curves were obtained by converting the original air design values to those of Freon-12 by assuming the same relative inlet and exit Mach numbers and flow angles at the mean radial station and the same relative inlet and exit angles at the tip and root. (See the appendix of ref. 2.)

Good agreement was obtained between rake and survey-probe total-pressure measurements as shown in figure 6(a). The slightly higher values obtained from the rake over the inner half of the annulus may be due to guide-vane wake carry through or to a nonuniform upstream total-pressure distribution. No attempt was made to survey circumferentially in order to determine the presence of a downstream guide-vane wake.

The measured total-pressure ratio was lower than estimated by about 8 percent at the root to about 30 percent at the tip, generally because of the combined effects of lower turning, higher relative exit Mach number, and lower relative total-pressure recovery than estimated. The smaller difference between estimated and measured values of total-pressure ratio at the root is attributed to the higher values of relative total-pressure recovery at that radial station. The higher values of relative pressure recovery at the root may be attributed to reduced boundary-layer separation in the blade passage because of the higher elemental mass flow in that region as shown in figure 6(d).

The relative exit Mach number (fig. 6(b)) was higher than estimated over most of the blade span because of poorer diffusion, and, when coupled with lower turning angles (fig. 6(c)), produced lower absolute exit Mach numbers. The portion of the blade where the relative inlet angle was equal to or greater than the estimated value had inlet Mach numbers high enough for an attached leading-edge shock, whereas the portion near the root operating at lower than design inlet angles was probably operating with a bow wave.

The effect of back pressure upon the compressor parameters at the mean radial station as functions of total-pressure ratio at design speed is presented in figure 7. The inlet conditions β_2 and M_2, which are expected to be independent of back pressure, were actually affected at the same total-pressure ratio as the decrease in weight flow shown in figure 5(b). Since the inlet conditions are determined independently from the Venturi tube, the decrease in inlet weight flow substantiates that measured by the Venturi tube. The relative exit Mach number decreased and the relative total-pressure recovery increased with increasing back pressure as expected for supersonic diffusers when the normal shock in the passage is moved upstream.

The diffuser performance of the pitch section as a function of the relative inlet Mach number is shown in figure 8. The data were obtained at the maximum total-pressure-ratio conditions over the range of tip speed tested. The ability to diffuse decreases very rapidly above a Mach number of 1.42 as evidenced by the sharp drop in both the relative total-pressure recovery and static-pressure rise.

Rotor Without Guide Vanes

Overall performance.- The overall performance of the rotor operating without guide vanes over the speed range tested is presented in figure 9 in terms of adiabatic efficiency and equivalent weight flow as functions of total-pressure ratio at constant speeds. At the design tip speed of 730 fps, a total-pressure ratio of 1.96 with an efficiency of 74.5 percent and a weight flow of 52 lb/sec of Freon-12 were measured. However, a peak pressure ratio of 2.0 with an efficiency of 81 percent and a weight flow of 51.2 lb/sec of Freon-12 was measured at 95 percent of design speed.

The effect of back pressure on weight flow at speeds above design was similar to that obtained with guide vanes. At design speed a small decrease in weight flow occurred at a pressure ratio of 1.85 and, although the weight flow increased slightly with further throttling, it did not again reach the value measured for the open-throttle condition as occurred with guide vanes. Unlike the rotor—guide-vane combination at design speed, there was no drop in efficiency at the point corresponding to the decrease in weight flow.

Over the entire speed range tested the rotor operating without guide vanes produced higher total-pressure ratios, efficiencies, and weight flows than the rotor with guide vanes except at the design speed of 730 fps where the pressure ratio and efficiency were lower. The cause of this drop at design speed is not known.

Rotor-blade-element performance.- Variations of several rotor parameters as functions of radial position at design speed and maximum efficiency are presented in figure 10.

The difference between rake and survey-probe total-pressure measurements (fig. 10(a)) was about the same as for the rotor—guide-vane combination. Since the instrument locations for the two series of tests were identical, this difference cannot be attributed to guide-vane wake but may have been caused by nonuniform upstream total-pressure distribution or misalinement of the survey probe due to an inward radial flow.

The total-pressure ratio and relative total-pressure recovery (fig. 10(a)) were about the same at the mean radial station but were lower at both the tip and root sections than for the rotor operating with guide vanes. The static-pressure rise was about the same near the hub where the relative inlet Mach numbers (fig. 10(b)) were about equal, but the rotor with no guide vanes produced a higher static-pressure rise over the rest of the blade because of higher inlet Mach numbers over the corresponding span.

Since the spanwise variation of relative inlet flow angle (fig. 10(c)) was similar to that obtained with guide vanes (because of higher axial velocities), the spanwise variation of angle of attack was also similar because of the fixed blade geometry.

Slightly lower turning angles (about 1° at the tip to 3.5° at the root) were obtained without guide vanes, and the absolute exit angles varied inversely with relative exit Mach numbers for the two operating conditions.

The absolute exit Mach numbers were lower than those obtained with guide vanes although the radial variations were similar to the rotor—guide-vane combination. As in the case of the rotor operating with guide vanes, the higher elemental mass flow near the root, which is caused by the inward flow necessary to set up simple radial equilibrium, produces higher absolute exit Mach numbers and total-pressure recoveries.

The effect of back pressure upon compressor parameters at the mean radial station at design speed is presented in figure 11 as functions of total-pressure ratio. The relative flow angle and Mach number (β_2 and M_2) were slightly higher than for the rotor—guide-vane combination as expected and showed a similar effect of throttle at about the same point as indicated by the Venturi tube in the weight flow of figure 9(b). The exit conditions were similar to those obtained for the rotor operating with guide vanes.

The diffuser performance of the pitch section as a function of relative inlet Mach number is shown in figure 12 for the maximum total-pressure ratio over the range of speed tested. Removal of the guide vanes produced better diffusion as evidenced by the higher static-pressure rise and total-pressure recovery.

Effect of Leading-Edge Radius

Because a guide-vane wake interfered with measurements of the performance of the rounded leading-edge blades (ref. 1) but not with the sharp leading-edge blades (fig. 6(a)) with the identical downstream instrumentation, it is felt that the differences in all parameters (except weight flow) obtained between the two sets of tests cannot be attributed solely to the leading-edge radius, but may be due to some extent to a circumferential shift in the guide-vane—wake carry through. Therefore, since it is not possible to determine to what extent these differences of the results between the two rotors operating with guide vanes are caused by the wake, a discussion of the leading-edge effects must be limited to the tests of the rotor without guide vanes. However, it should be pointed out that the results of the rotor—guide-vane combinations show similar trends for all parameters except at design speed without guide vanes.

Overall performance.- The effects of rounding the leading edge on the overall performance of the rotor without guide vanes can be seen from figure 9. The dashed-line curve is an envelope of the maximum efficiencies obtained from figure 12 of reference 1. From a comparison of the two envelope curves, it can be seen that rounding the leading edge decreased both the total-pressure ratio and efficiency from about 1 percent at 515 fps to 6 percent at 815 fps. At the design speed of 730 fps, the rounded leading-edge blades decreased the efficiency by 4 percent but produced a 5-percent-higher total-pressure ratio. However, this higher value of total-pressure ratio was not always reached with the rounded leading-edge rotor because of the peculiar operation which is described in reference 1.

A comparison of the surge lines (fig. 9(b)) shows that at speeds up to 590 fps both sets of blades produced about the same weight flow at full throttle. This may possibly be due to the fact that at those lower speeds the sharp-edged blades also operated with a detached shock. However, at speeds above 590 fps, rounding the leading edges decreased the weight flow at closed throttle about 5 percent. This decrease is attributed to the higher losses due to a stronger upstream bow-wave pattern caused by the rounded leading edge. The effect of back pressure on weight flow at speeds above design was similar for both rotors, but at the design speed of 730 fps the weight flow was independent of back pressure only for the rounded leading-edge blades. No explanation can be given at this time for the difference in the characteristic curves at design speed.

The variation of weight-flow range with equivalent tip speed for the two sets of blades is presented in figure 13 where the range parameter is the ratio of the difference in weight flow at open and closed throttle to the weight flow at open throttle. Contrary to expectations, the sharp-edged rotor had a wider operating range than the rounded leading-edge rotor with the greatest difference at the lower speeds where the tip Mach number was about 1.1.

Rotor-blade-element performance.- In general, the trends of all parameters are similar for both sets of blades (fig. 10). Although rounding the leading edges decreased the relative total-pressure recovery by about 5 percent, it produced a higher total-pressure ratio. This higher pressure ratio, which occurred only at this speed, was apparantly due to both higher turning and lower relative exit Mach number. The lower axial velocity obtained with the rounded leading-edge blades caused the rotor to operate at a higher angle of attack and a lower relative inlet Mach number and to produce a lower weight flow.

A comparison between the two rotors of the effect of back pressure on the parameters at the pitch section shows trends similar to those observed at all radial stations. The parameters whose differences between the two rotors were most affected by throttle were absolute exit Mach number and turning angle.

A comparison of the diffuser performance of the pitch sections of the two sets of blades (fig. 12) shows that rounding the leading edges caused poorer diffusion as evidenced from the decrease in both relative total-pressure recovery and static-pressure rise. Rounding the leading edges reduced the relative total-pressure recovery from 2.5 percent at an inlet Mach number of about 1.0 to about 12 percent at a Mach number of 1.55. According to the cascade analysis of reference 4, the maximum loss due to an upstream bow wave for the 0.010-inch leading-edge radius of these blades should be about 1.5 percent at the highest Mach number reached. Therefore, the higher losses obtained for this rotor from rounding the leading edges must be attributed to the changes in the shock boundary-layer interaction caused by the wave patterns set up within the blade passages. This appears to be further substantiated from a comparison of the variation of relative total-pressure recovery of figure 10. Although only the sharp-edged rotor operated with an attached shock at the tip section, whereas both rotors had a detached bow wave at the root section (determined from the inlet Mach number and angle for a given leading-edge wedge angle), the difference in relative total-pressure recovery between the two sets of blades at these radii are about the same.

CONCLUSIONS

An experimental investigation has been conducted in Freon-12 of a shock-in-rotor-type axial-flow supersonic compressor having sharp leading-edge blades with an 8-percent mean thickness-chord ratio. The data obtained were compared with those of the rounded leading-edge rotor of NACA RM L53G16. The following conclusions have been obtained:

1. The rotor operating with guide vanes at a design speed of 730 fps produced a total-pressure ratio of 2.06 and an efficiency of 78.6 percent with a weight flow of 51.2 lb/sec of Freon-12.

2. The rotor operating without guide vanes produced a total-pressure ratio of 1.96 and an efficiency of 74.5 percent with a weight flow of 52 lb/sec of Freon-12 at design speed but reached a peak pressure ratio of 2.0 and an efficiency of 81 percent with a weight flow of 51.2 lb/sec of Freon-12 at 95 percent of design speed.

3. At design speed and above for both configurations, the mass flow was affected by back pressure.

4. The total-pressure ratio, efficiency, and weight flow decreased sharply at speeds above design.

5. Rounding the leading edges decreased the relative total-pressure recovery probably a result of changing the shock boundary-layer interaction caused by a changing wave pattern within the blade passage.

6. Rounding the leading edges decreased the total-pressure ratio, efficiency, and weight flow at all speeds and configurations except at the design speed without guide vanes at which point a higher total-pressure ratio was reached.

7. Rounding the leading edges decreased the inlet axial velocity which increased the angle of attack and decreased the inlet Mach number and weight flow.

8. Rounding the leading edges reduced the weight-flow range over the entire speed range tested.

Langley Aeronautical Laboratory,
National Advisory Committee for Aeronautics,
Langley Field, Va., October 28, 1954.

REFERENCES

1. Goldberg, Theodore J., Boxer, Emanuel, and Bernot, Peter T.: Experimental Investigation of an Axial-Flow Supersonic Compressor Having Rounded Leading-Edge Blades With an 8-Percent Mean Thickness-Chord Ratio. NACA RM L53G16, 1953.

2. Boxer, Emanuel, and Erwin, John R.: Investigation of a Shrouded and an Unshrouded Axial-Flow Supersonic Compressor. NACA RM L50G05,1950.

3. NACA Subcommittee on Compressors: Standard Procedures for Rating and Testing Multistage Axial-Flow Compressors. NACA TN 1138, 1946.

4. Klapproth, John F.: Approximate Relative-Total-Pressure Losses of an Infinite Cascade of Supersonic Blades With Finite Leading-Edge Thickness. NACA RM E9L21, 1950.

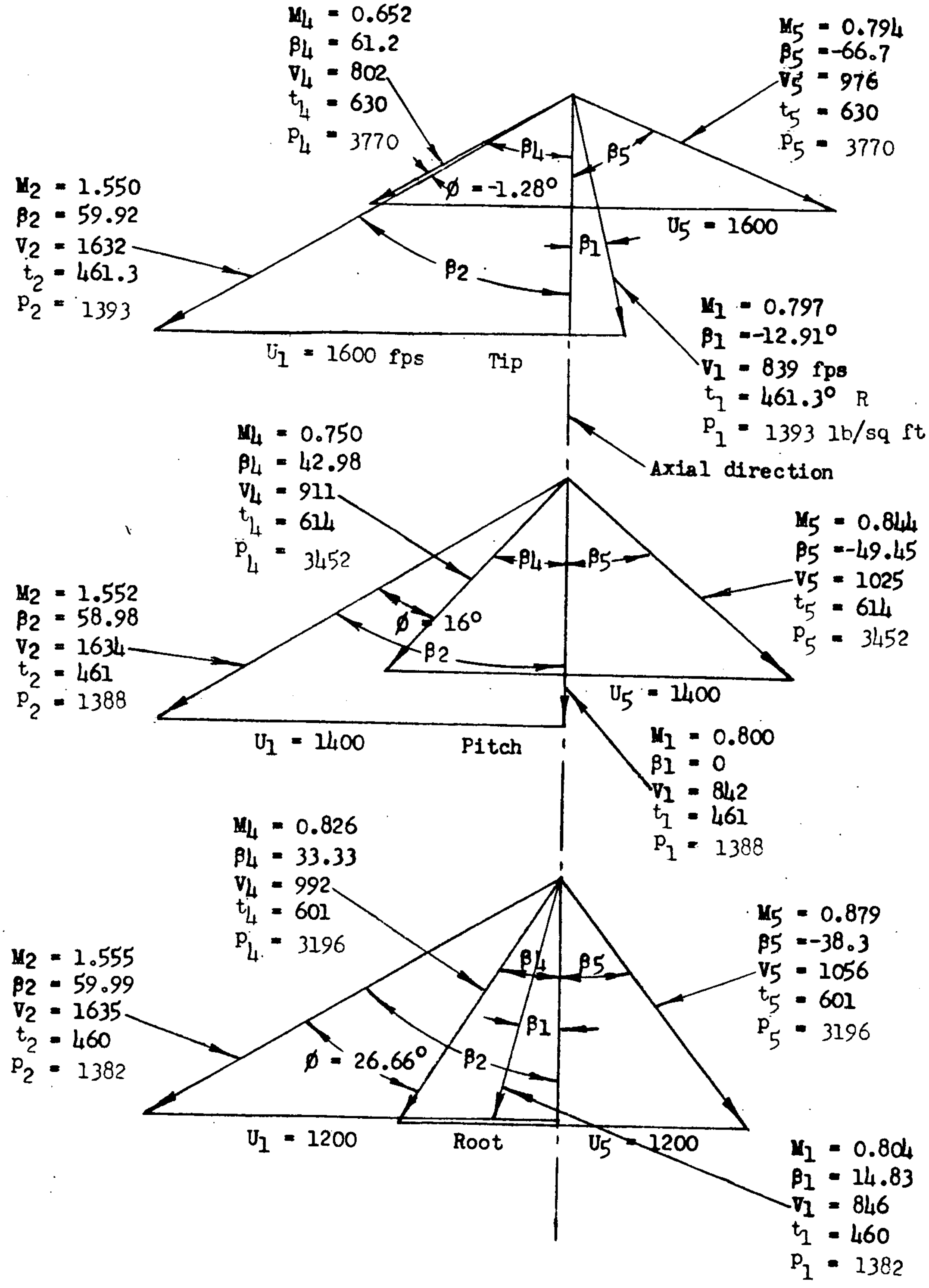

Figure 1.-Supersonic-compressor velocity diagrams for the tip, pitch, and root sections in air. Initial conditions, P_o = 1.0 atmosphere; T_o = 520° F absolute.

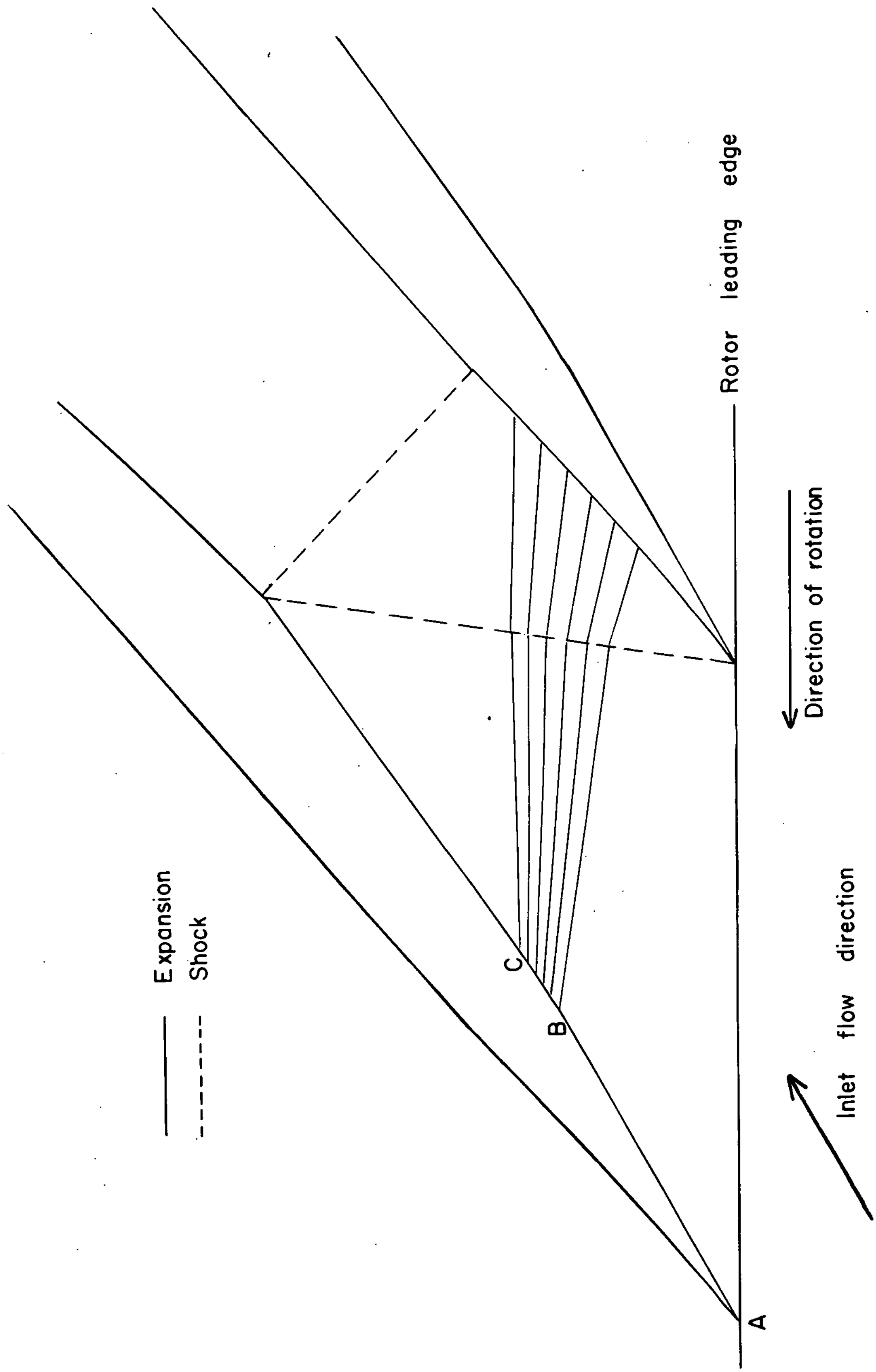

Figure 2.- Supersonic portion of a two-dimensional rotor blade.

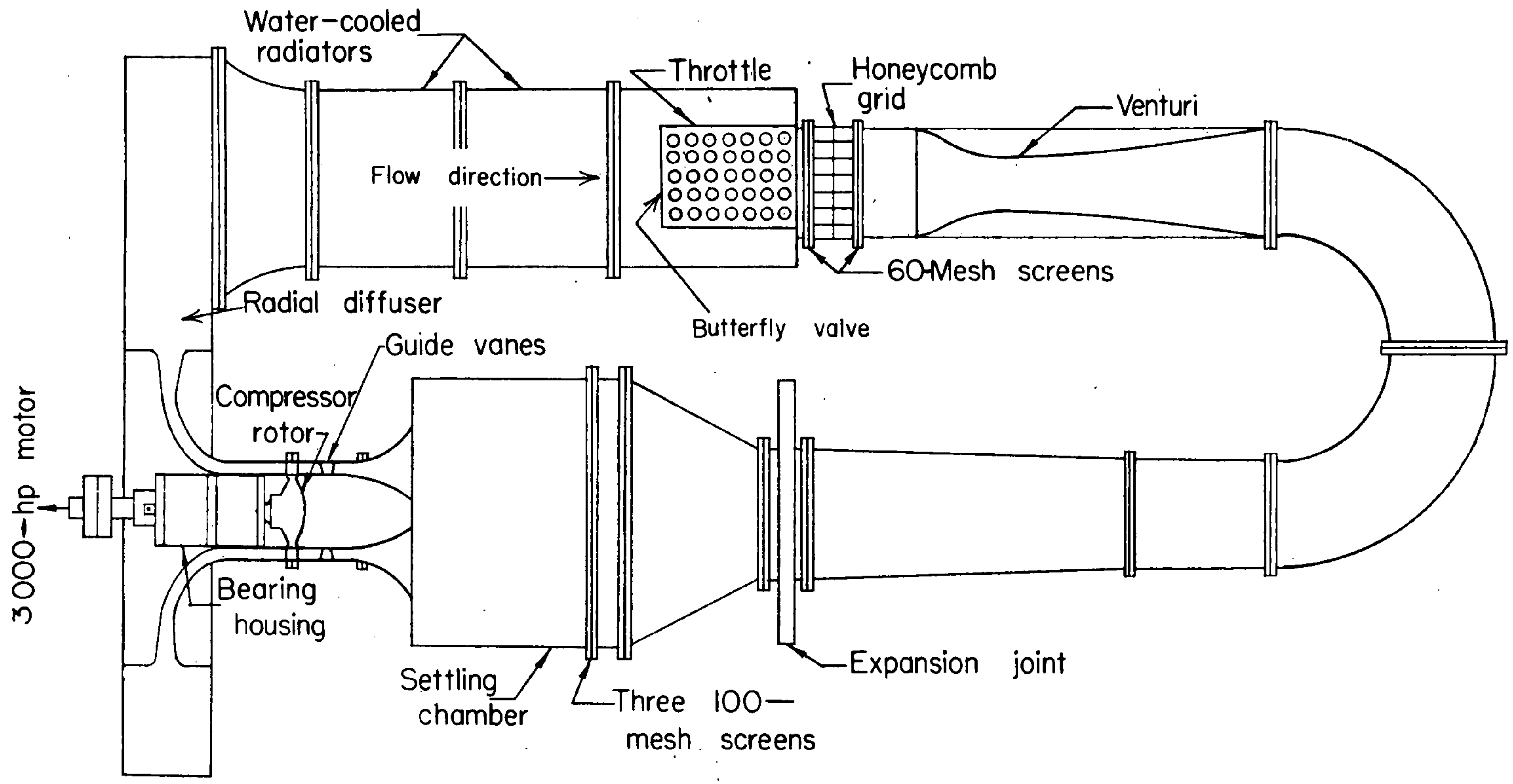

Figure 3.- Schematic arrangement of supersonic-compressor test rig.

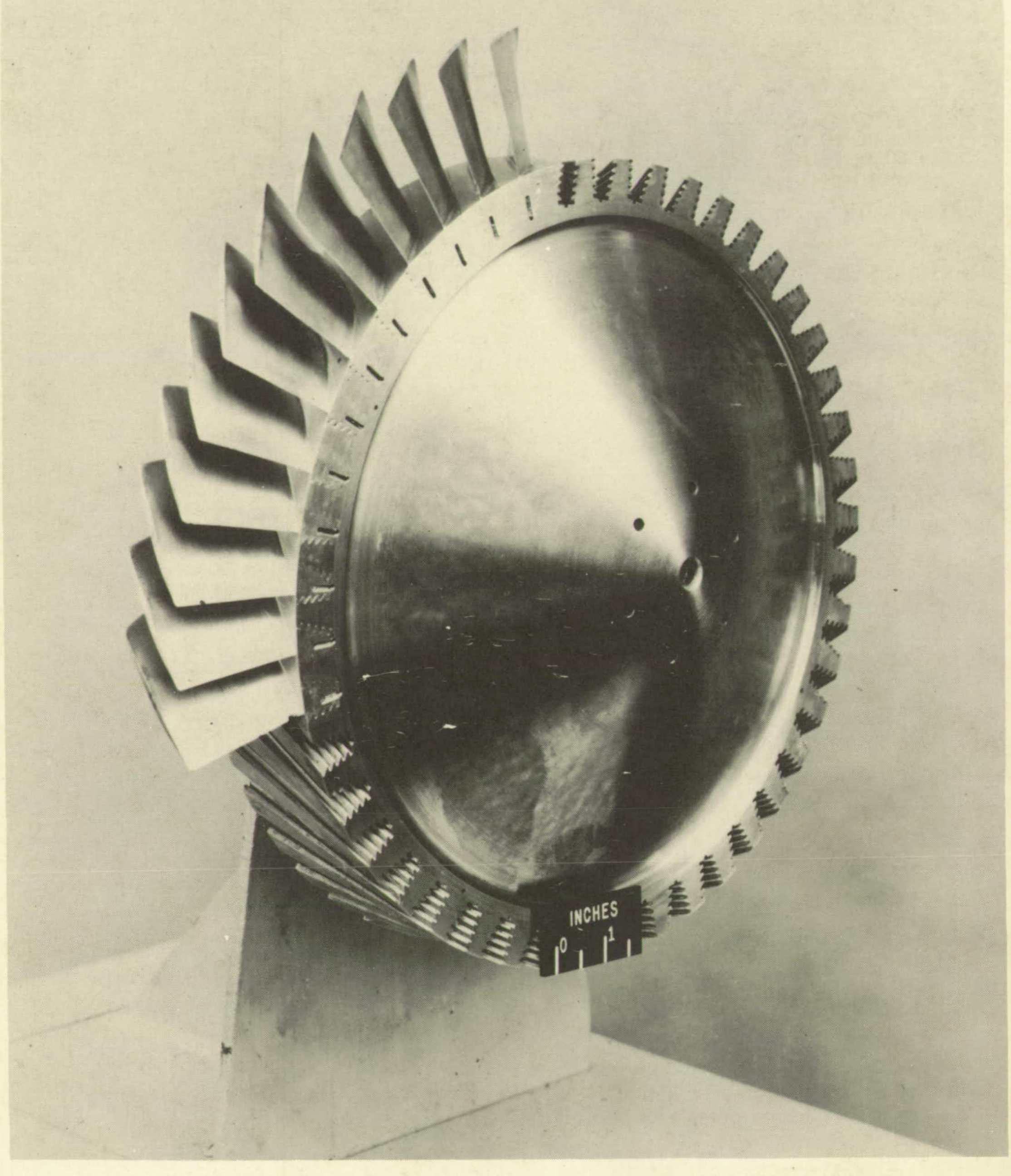

L-86020

Figure 4.- Test rotor partly assembled.

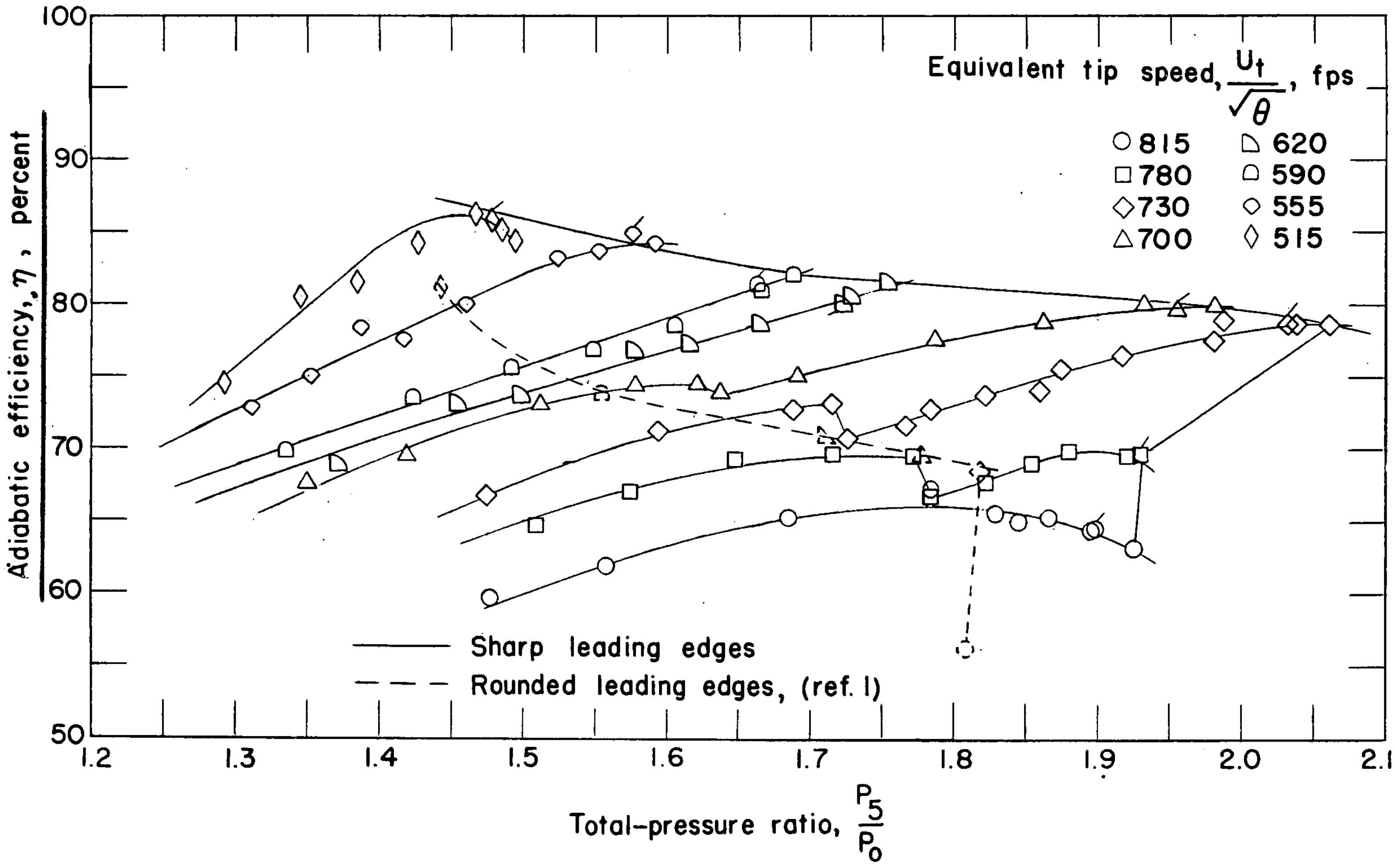

(a) Total-pressure ratio against efficiency.

Figure 5.- Rotor characteristics with guide vanes. Results were obtained in Freon-12. Flagged symbols represent mass-weighted values.

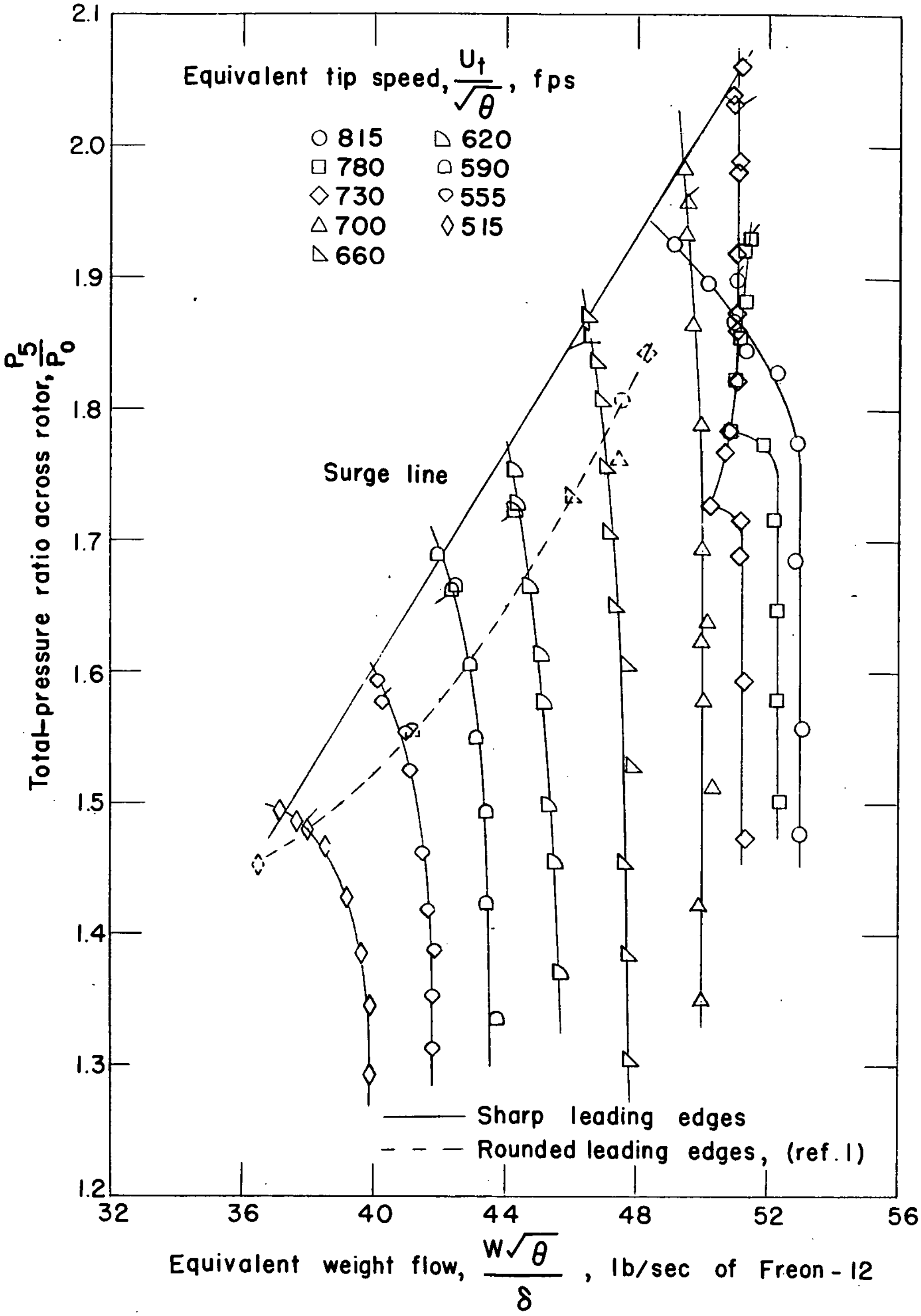

(b) Total-pressure ratio against weight flow.

Figure 5.- Concluded.

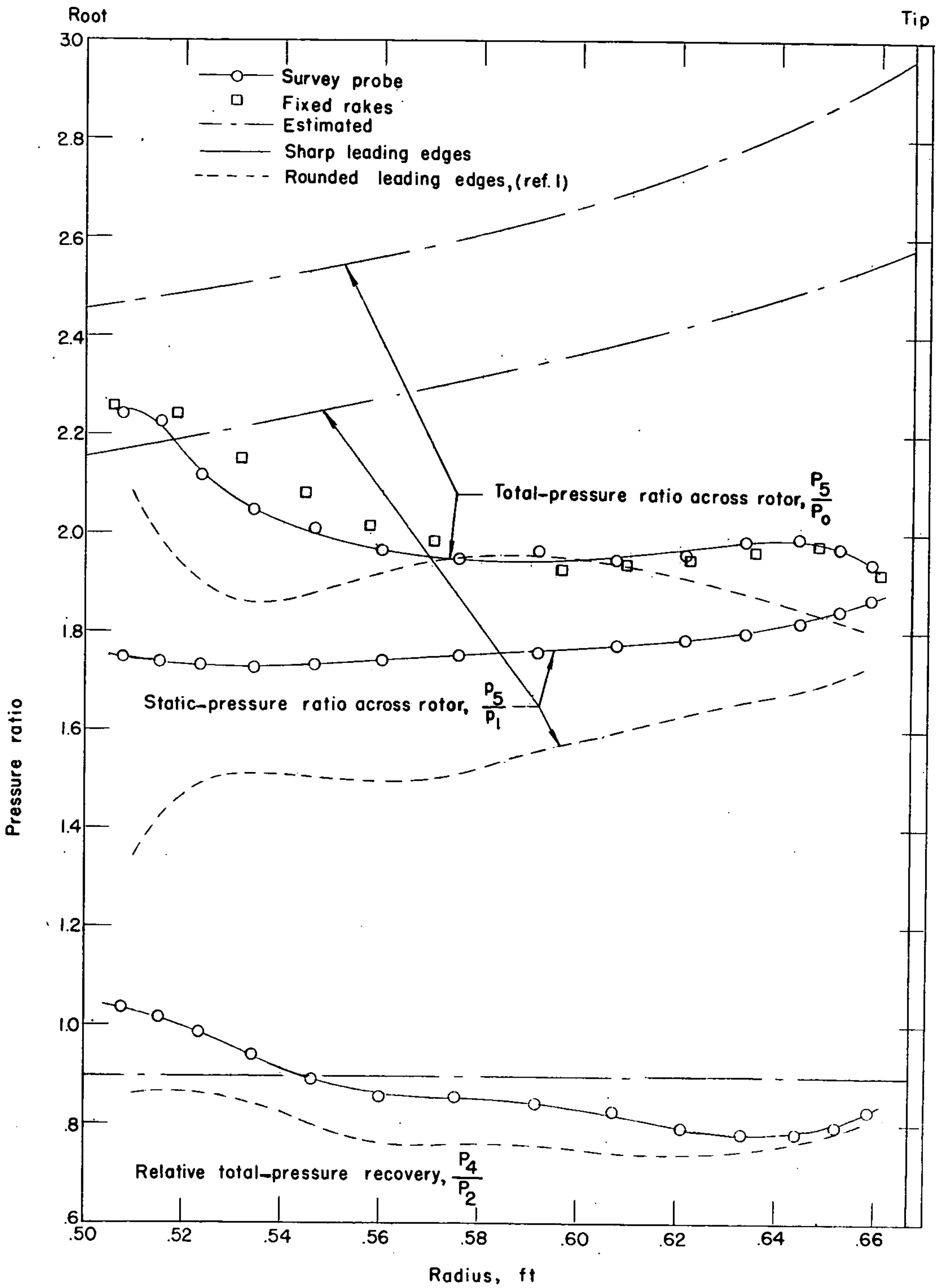

(a) Pressure-ratio distribution.

Figure 6.- Radial variation of compressor parameters at an equivalent tip speed of 730 fps in Freon-12 with guide vanes.

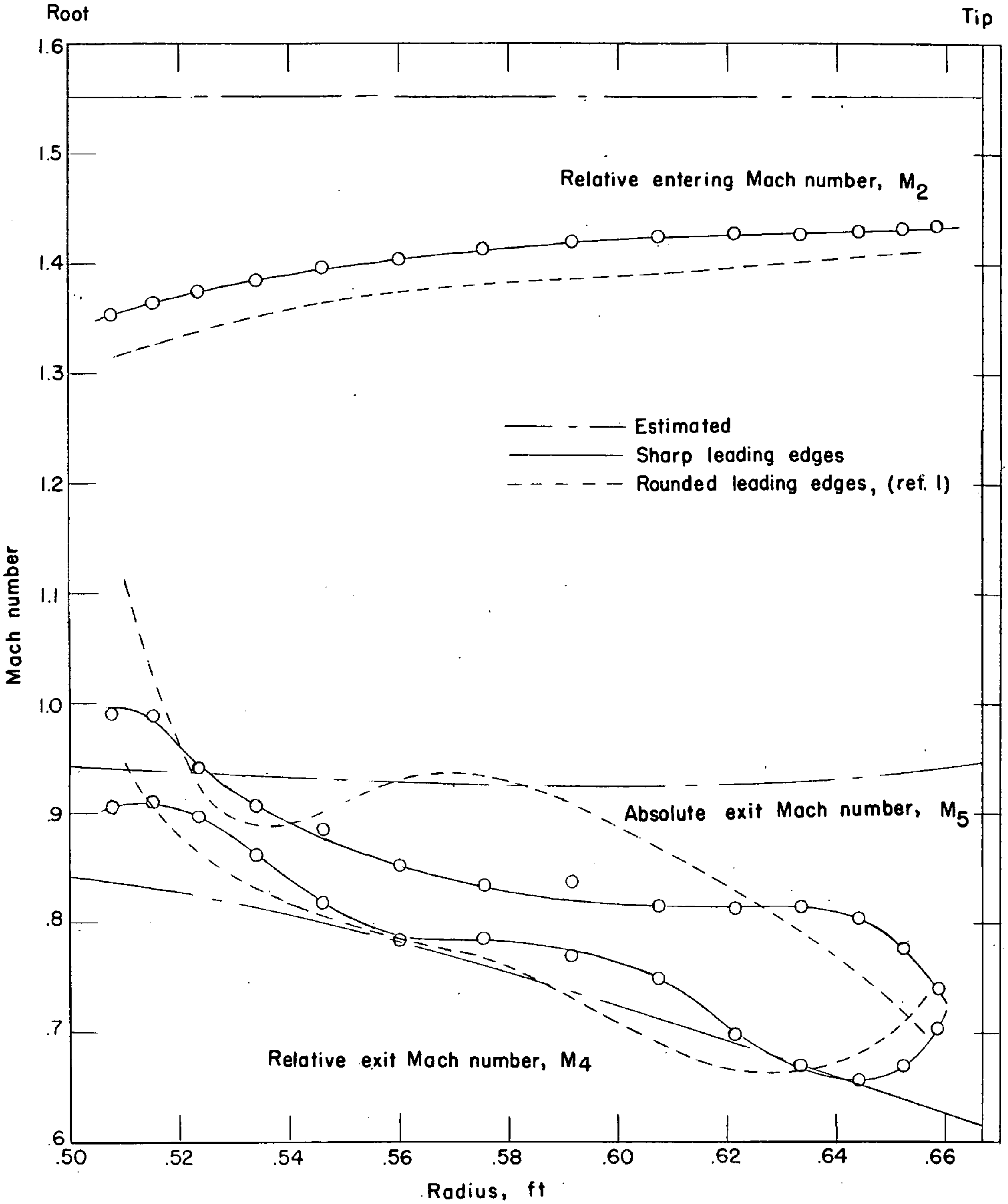

(b) Mach number distribution.

Figure 6.- Continued.

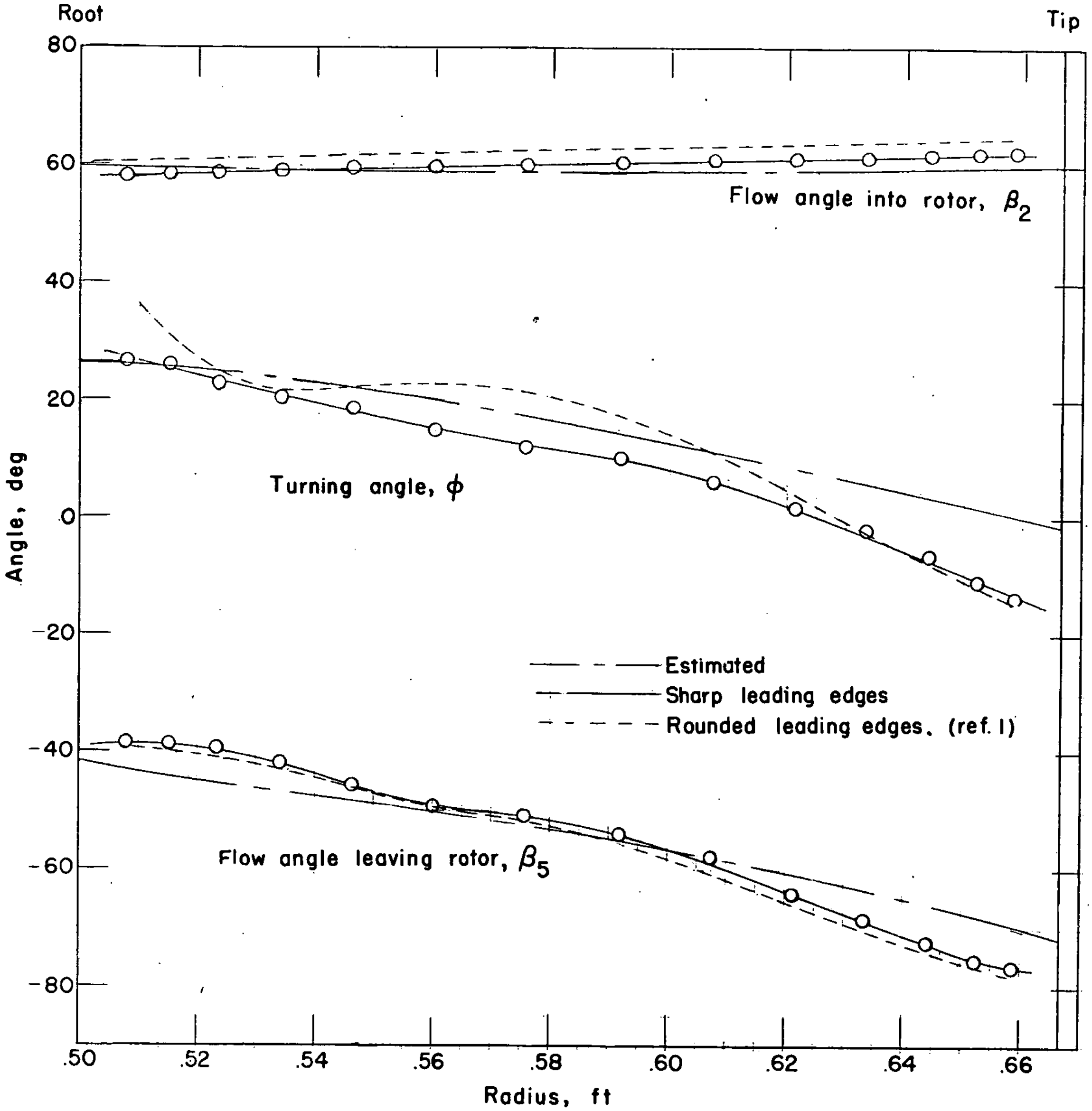

(c) Angle distribution.

Figure 6.- Continued.

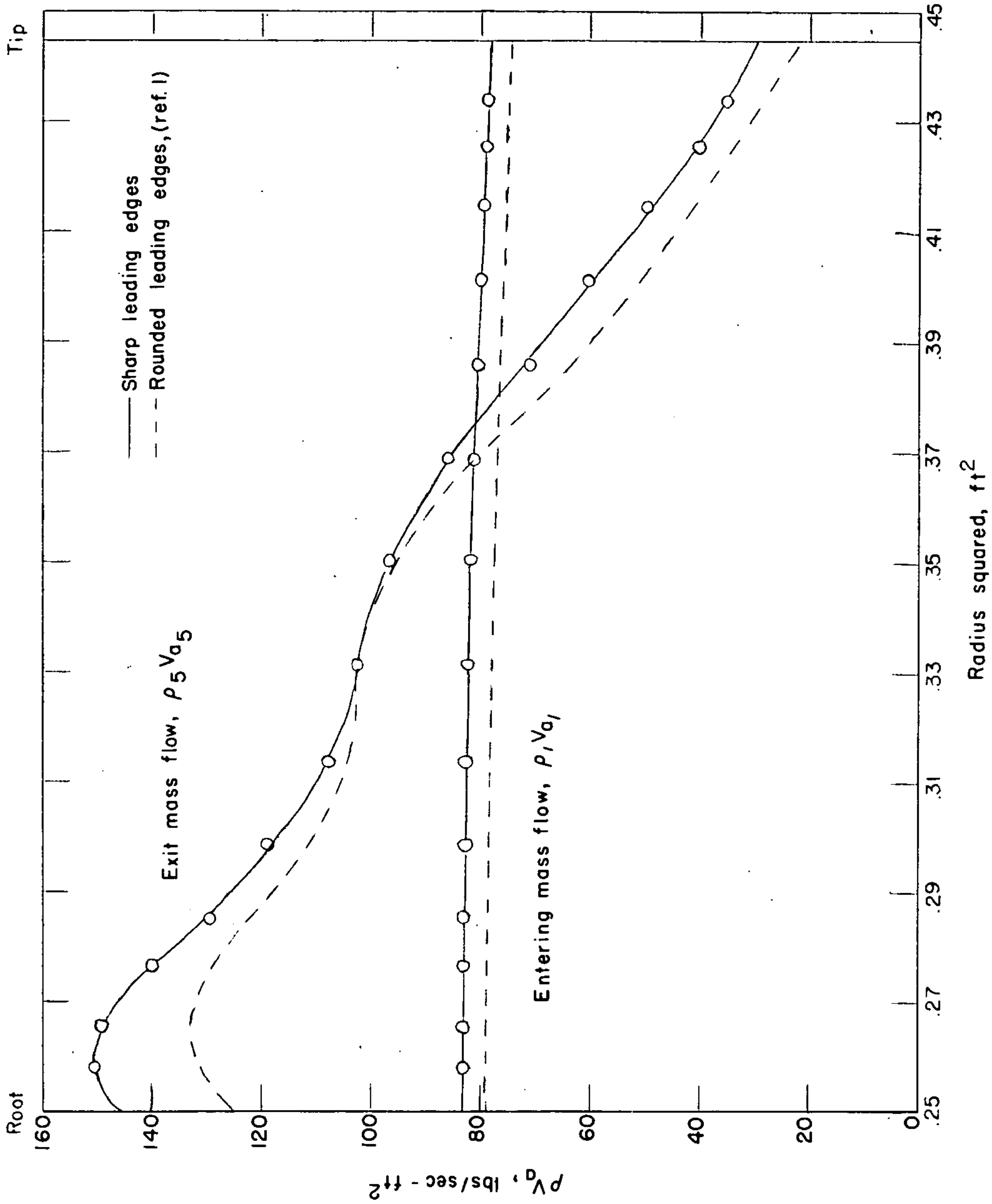

(d) Equivalent mass-flow distribution.

Figure 6.- Concluded.

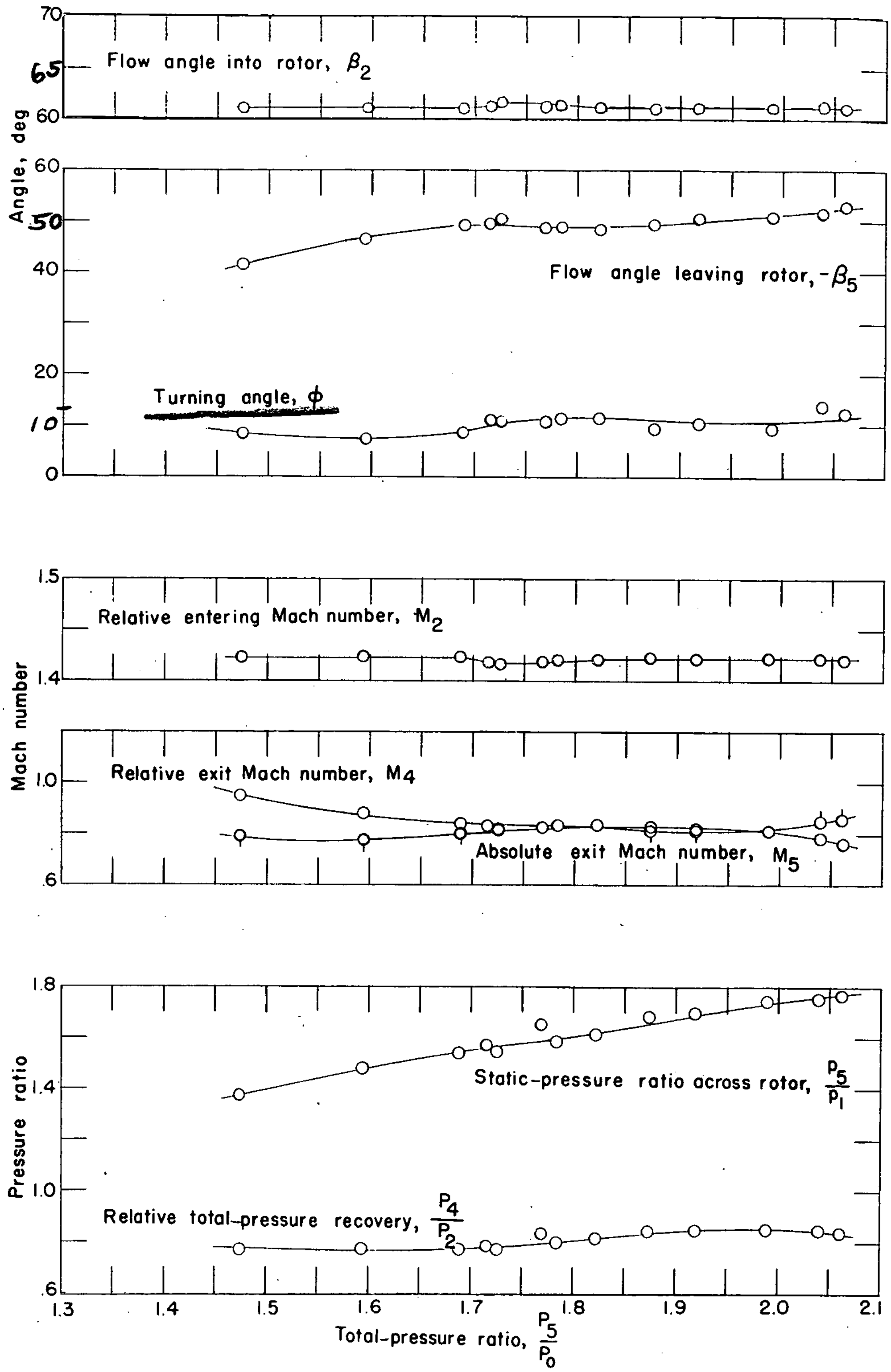

Figure 7.- Effect of throttle on compressor parameters at mean radius at an equivalent tip speed of 730 fps in Freon-12 with guide vanes.

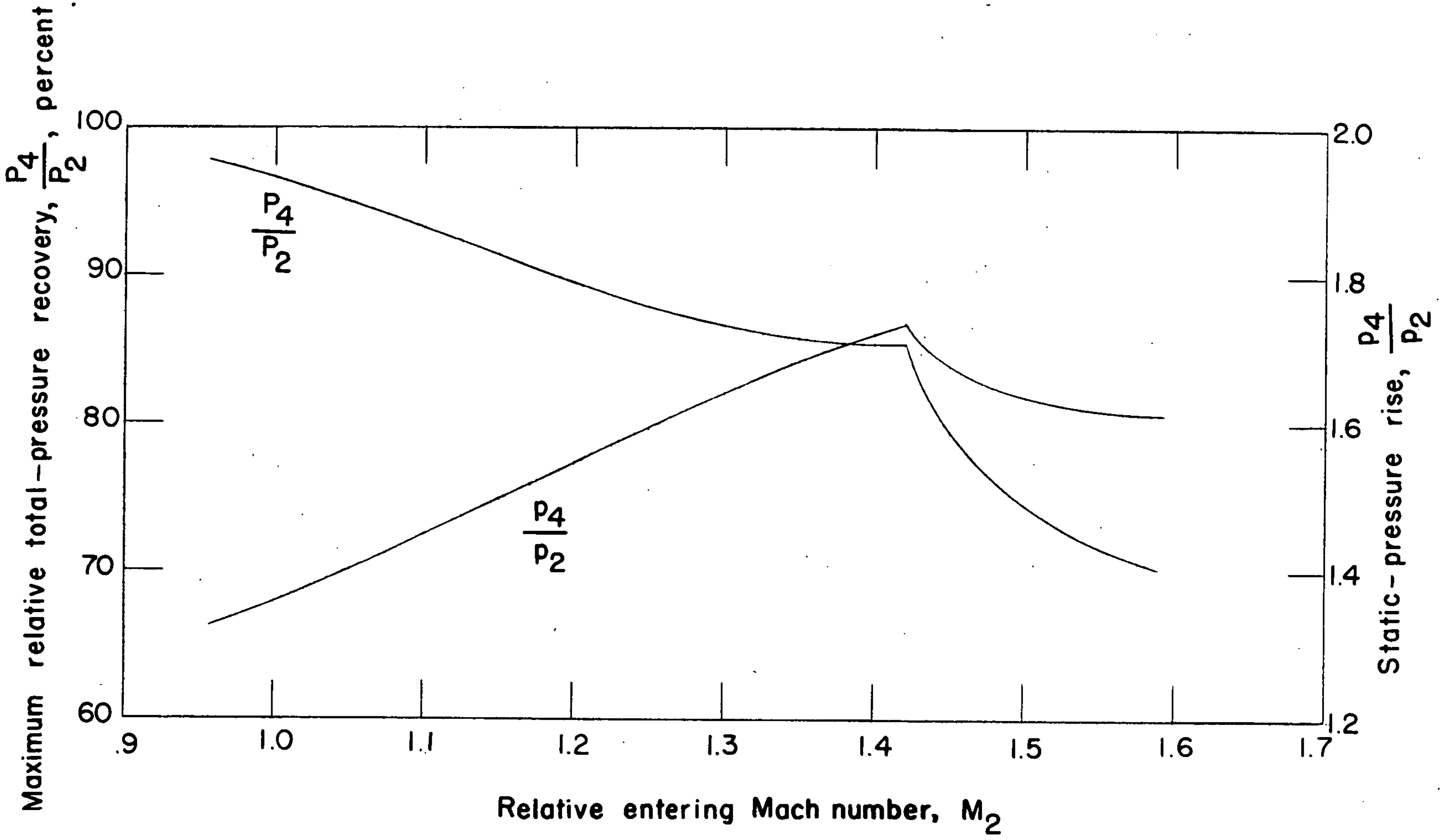

Figure 8.- Variation of maximum relative total-pressure recovery and static-pressure rise with relative inlet Mach number measured at the mean radius (with guide vanes).

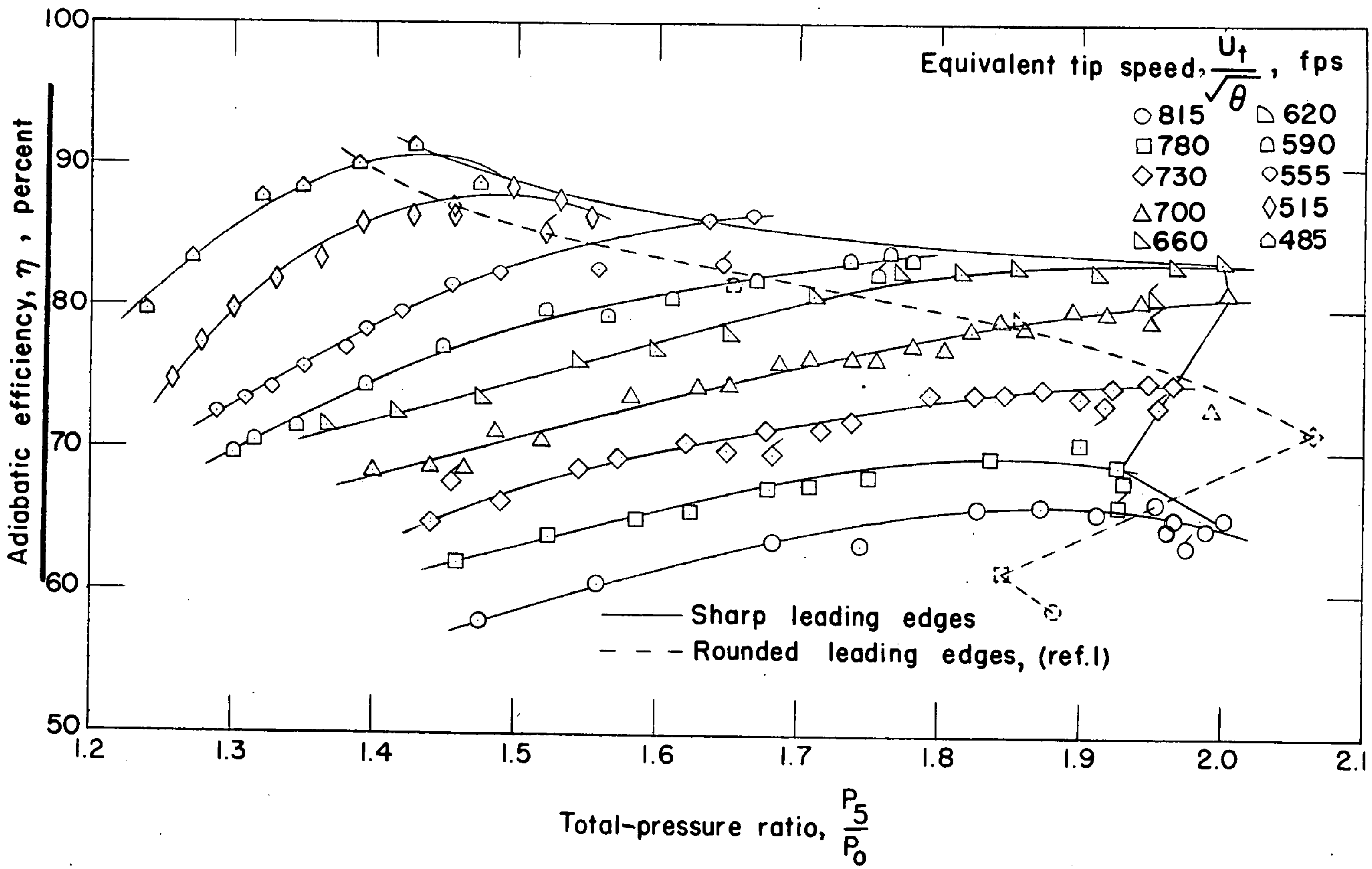

(a) Total-pressure ratio against efficiency.

Figure 9.- Rotor characteristics without guide vanes. Results were obtained in Freon-12. Flagged symbols represent mass-weighted values.

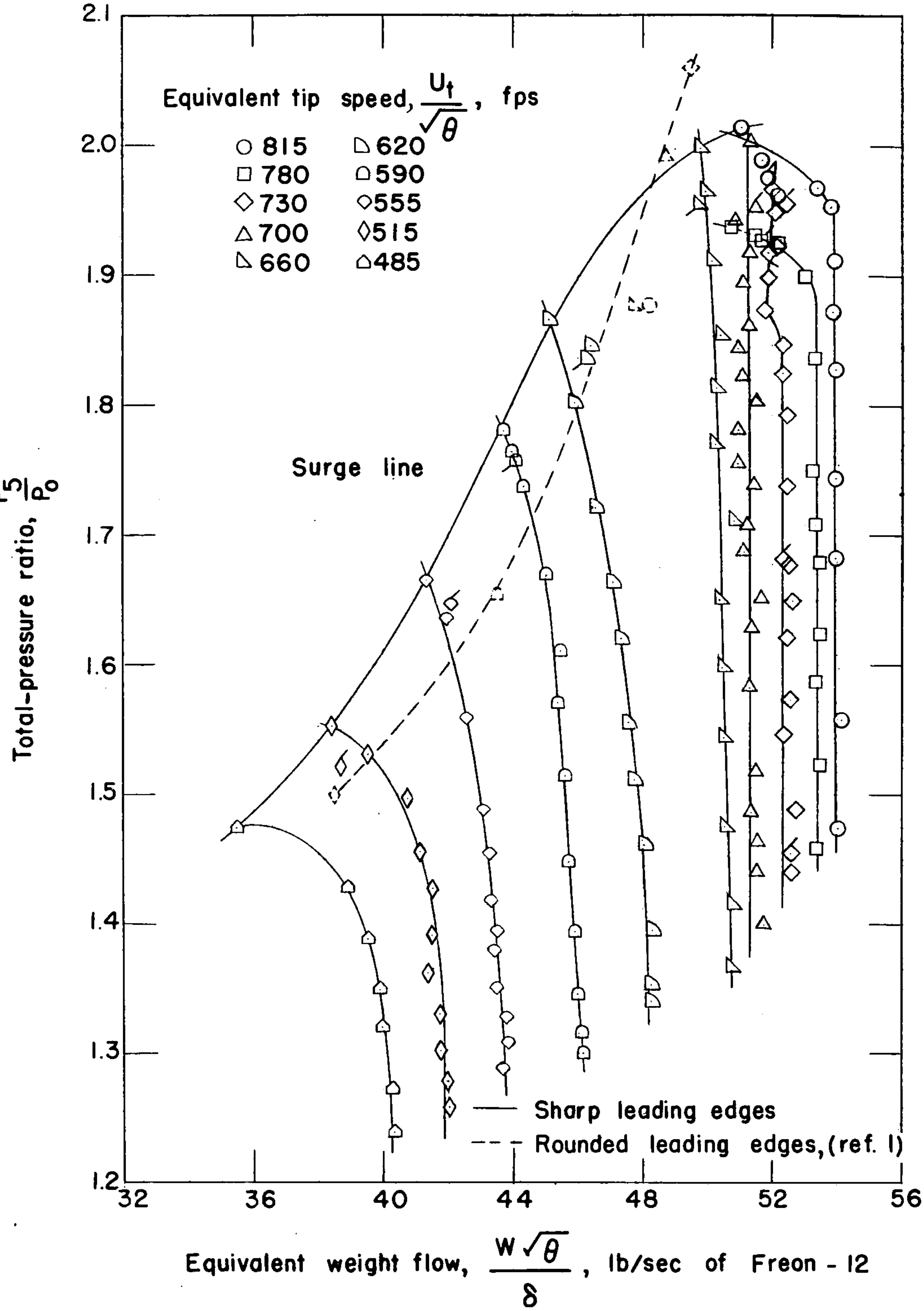

(b) Total-pressure ratio against weight flow.

Figure 9.- Concluded.

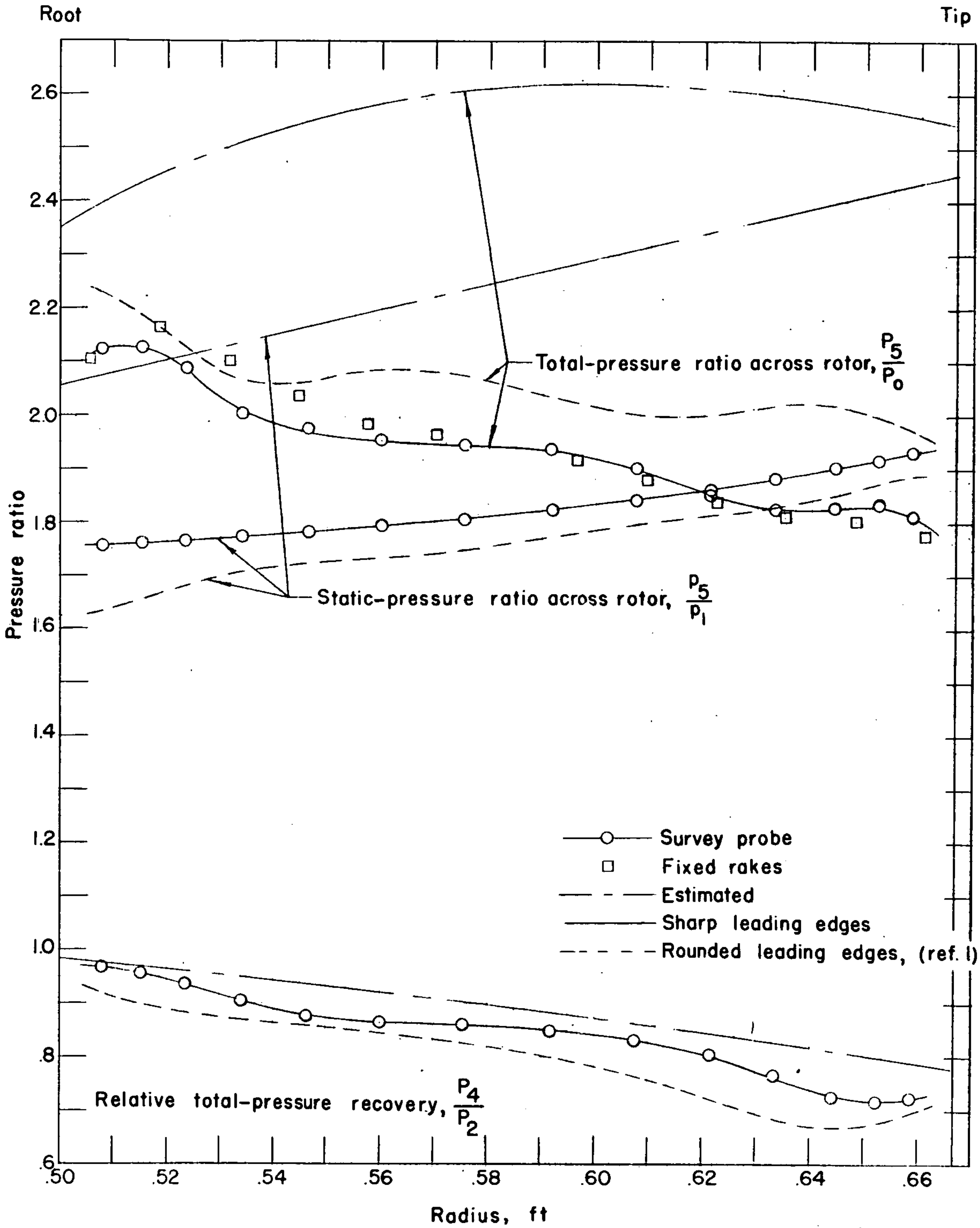

(a) Pressure-ratio distribution.

Figure 10.- Radial variation of compressor parameters at an equivalent tip speed of 730 fps in Freon-12 without guide vanes.

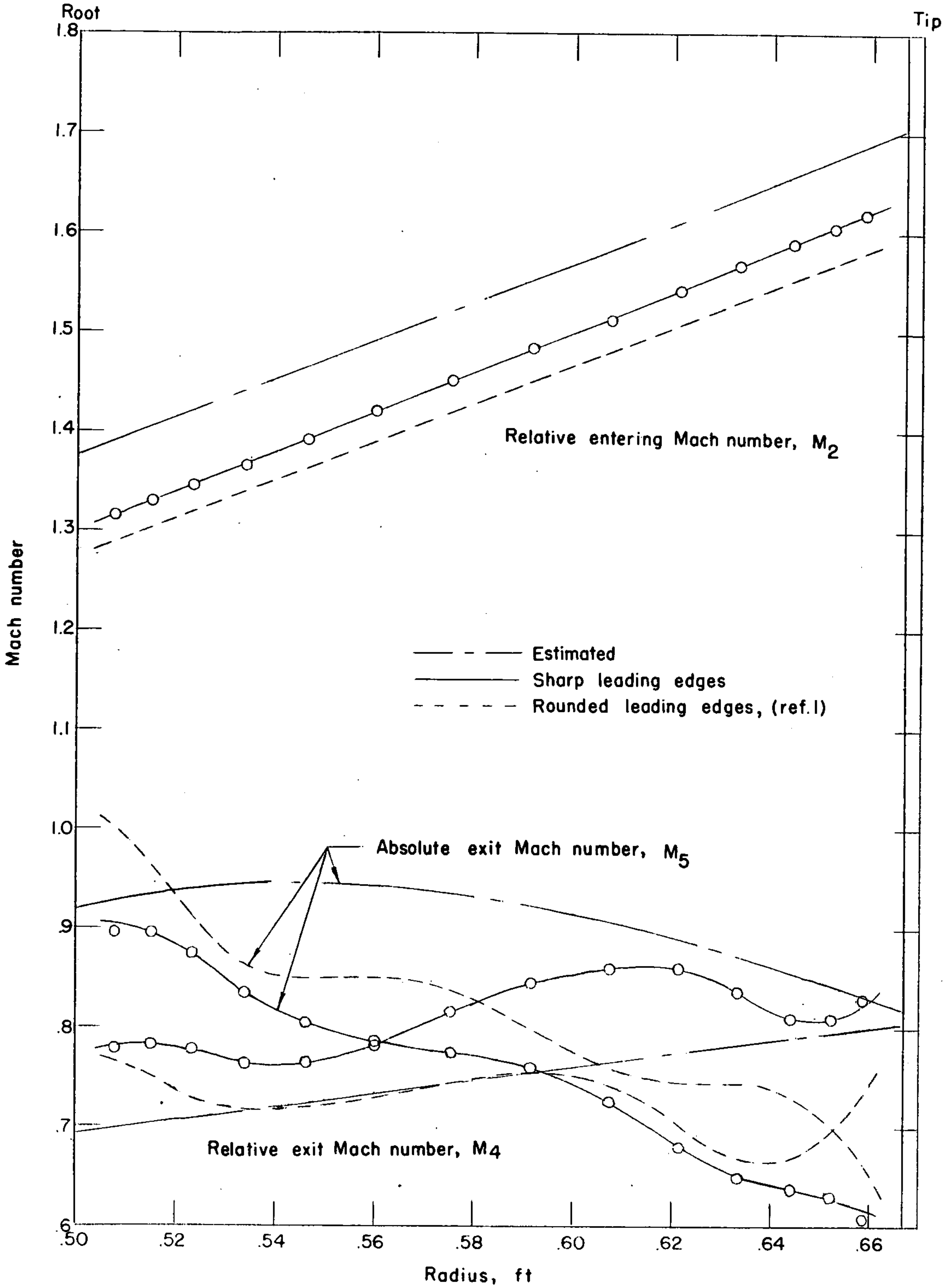

(b) Mach number distribution.

Figure 10.- Continued.

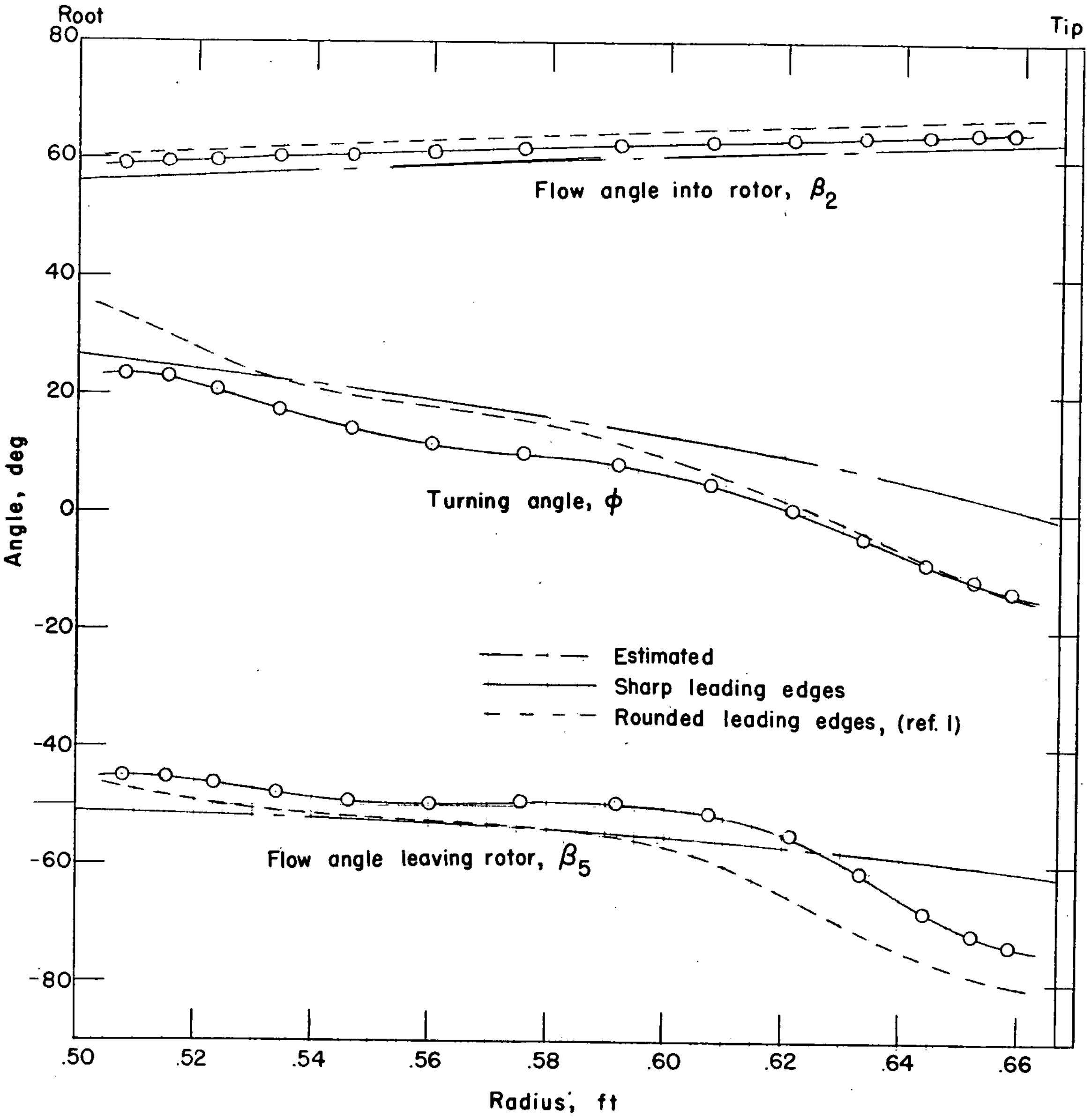

(c) Angle distribution.

Figure 10.- Continued.

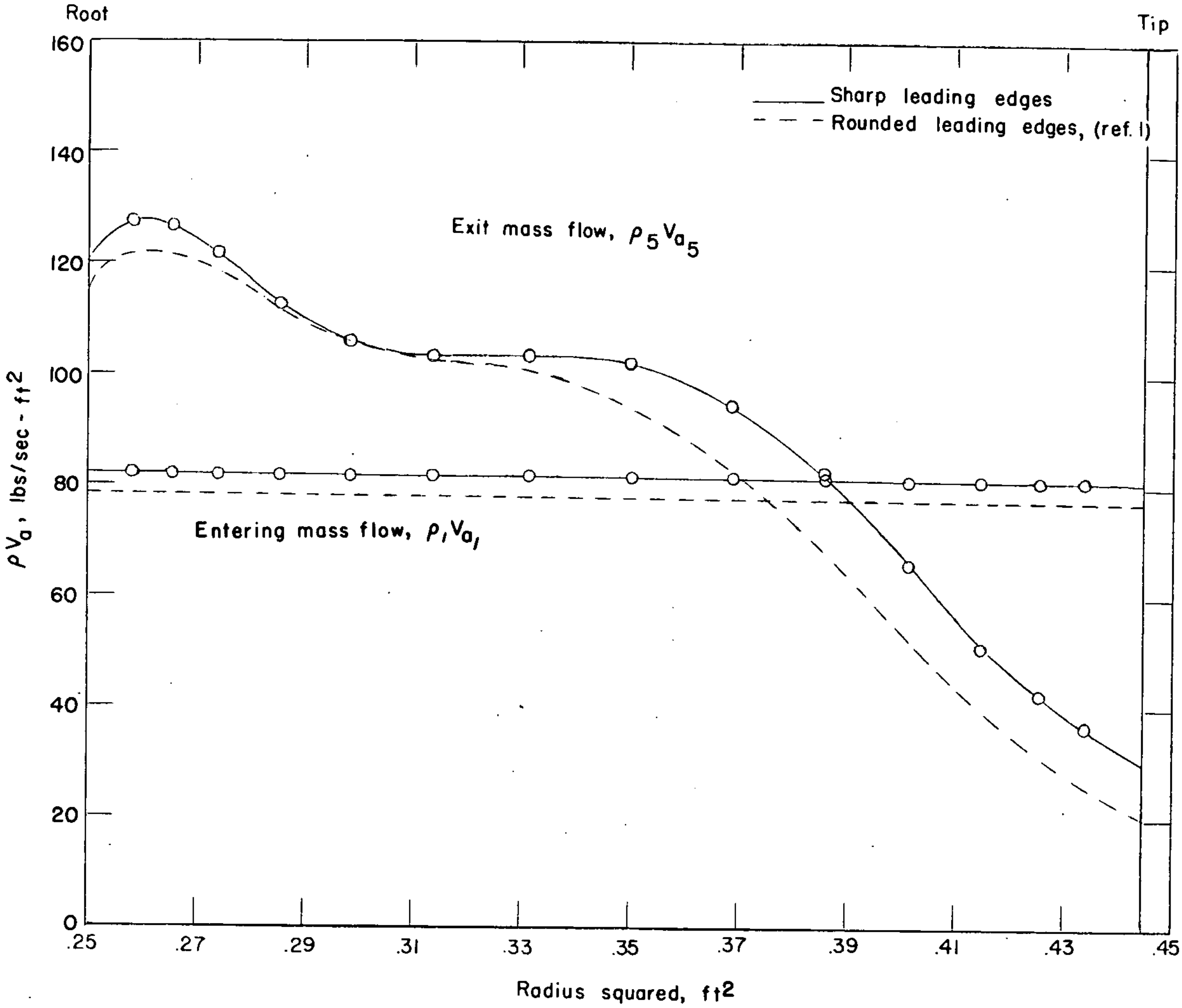

(d) Equivalent mass-flow distribution.

Figure 10.- Concluded.

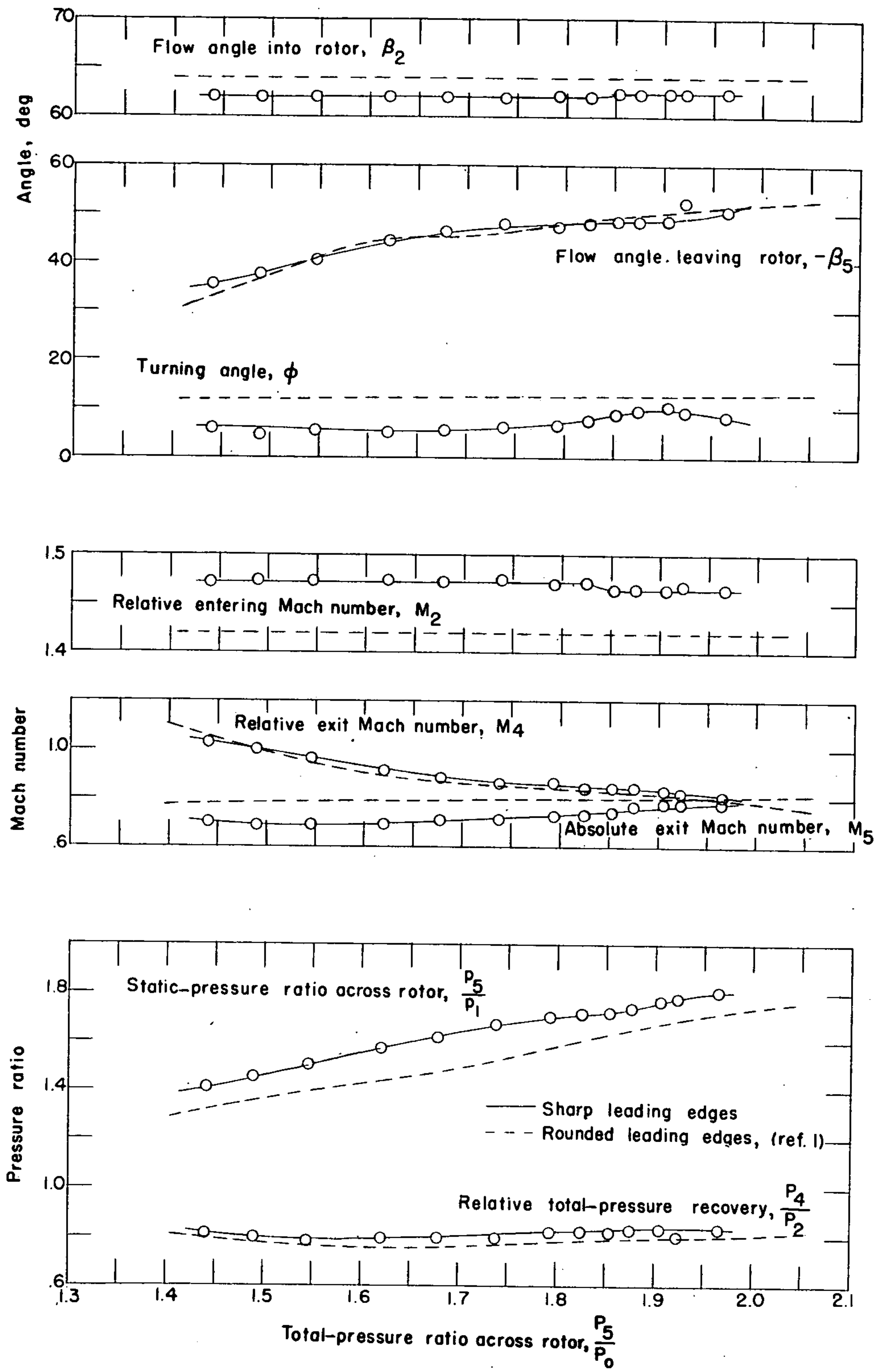

Figure 11.- Effect of throttle on compressor parameters at mean radius at an equivalent tip speed of 730 fps in Freon-12 without guide vanes.

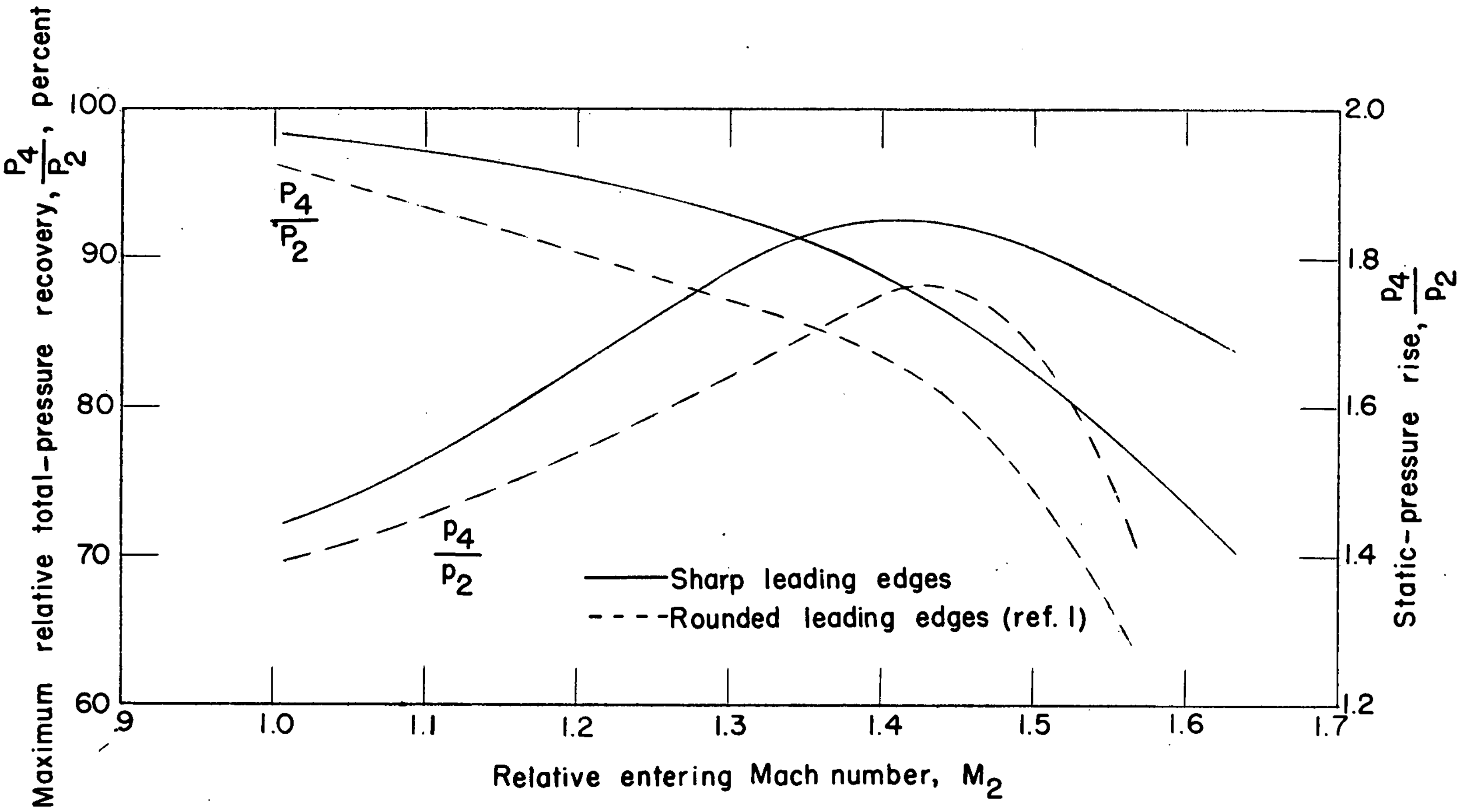

Figure 12.- Variation of maximum relative total-pressure recovery and static-pressure rise with relative inlet Mach number measured at the mean radius (without guide vanes).

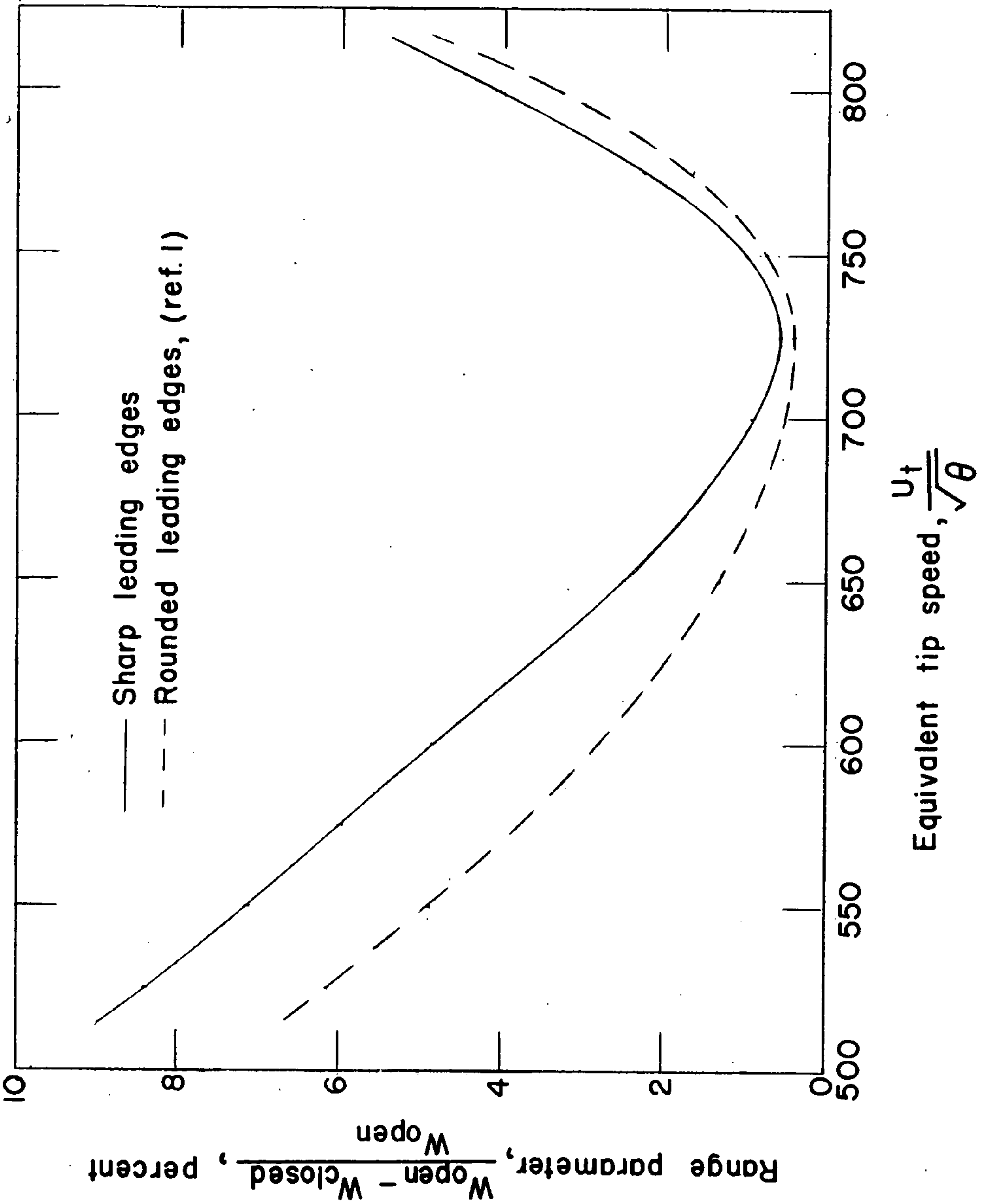

Figure 13.- Variation of weight-flow range with equivalent tip speed (without guide vanes).